

Landau levels in the case of two degenerate coupled bands: Kagomé lattice tight-binding spectrum

Yi Xiao, Vincent Pelletier, Paul M. Chaikin, and David A. Huse
Department of Physics, Princeton University, Princeton, New Jersey 08544
 (Received 21 October 2002; published 7 March 2003)

The spectrum of charged particles hopping on a kagomé lattice in a uniform transverse magnetic field shows an unusual set of Landau levels at low field. They are unusual in two respects: the lowest Landau levels are *paramagnetic* so their energies *decrease* linearly with increasing field magnitude, and the spacings between the levels are not equal. These features are shown to follow from the degeneracy of the energy bands in zero magnetic field. We give a general discussion of Landau levels in the case of two degenerate bands and show how the kagomé lattice tight-binding model includes one special case of this more general problem. We also discuss the consequences of this for the behavior of the critical temperature of a kagomé grid superconducting wire network, which is the experimental system that originally motivated this work.

DOI: 10.1103/PhysRevB.67.104505

PACS number(s): 74.81.-g

I. INTRODUCTION

The behavior of electrons in a two-dimensional periodic structure immersed in an external magnetic field has been a subject of special interest over the past two decades ever since Hofstadter's graphical solution for square lattice.¹ The competition between the periodic potential imposed by the lattice structure and the length scale provided by the magnetic field leads to frustration in the system and to intricate, detailed, and self-similar features for the subband spectrum of single-particle eigenenergies. The magnetic-field-induced frustration in two-dimensional structures has also been a subject of active experimental study using superconducting wire networks,^{2,3} as the linearized Ginzburg-Landau equation for the superconductor and the Schrödinger equation for the tight-binding electron wave function in these lattices share the same form.⁴ The investigation of a variety of structures, such as the triangular lattice,⁵ the honeycomb lattice,⁶ and recently the T_3 or dice lattice,^{7,8} has revealed the richness and the beauty of physics in these systems.

In this paper, we present our study of the Landau subband spectrum of the kagomé lattice, whose distinguishing degenerate ground state has attracted extensive attention over the last decade. The kagomé lattice is a two-dimensional lattice of corner-sharing triangles [Fig. 1(a)]. The nearest-neighbor-coupled Heisenberg antiferromagnet system on a kagomé lattice has been shown to have an infinite number of classical ground states, which give rise to a zero-temperature extensive entropy.^{9,10} However, this degeneracy may be partially lifted by quantum or thermal fluctuations.^{11–13} This so-called *order from disorder* mechanism¹⁴ selects the states with the largest fluctuations (thus the highest entropy or the lowest zero-point energy), which often are more ordered states.

Experimentally, kagomé systems have been previously studied in the context of adsorbed ^3He on graphite at millikelvin temperature^{9,15,16} and the layered oxide $\text{SrCr}_{8-x}\text{Ga}_{4+x}\text{O}_{19}$.^{10,17} Our recent experimental studies¹⁸ of nearly perfect kagomé structures using superconducting wire networks show interesting and complex phase boundaries between the normal and superconducting states, which agree well with Lin and Nori's mean-field calculation based on quantum interference.¹⁹ This work shows that a frustrated

ground state exists at a magnetic field of one-half of a flux quantum per triangular plaquette.

The lowest-energy states of a charged particle in a nondegenerate band become Landau levels when a small magnetic field B is added. The energies of these Landau levels *increase* linearly in $|B|$; the currents in these states are *diamagnetic*. The consequence of this for the critical temperature T_c of a periodic superconducting grid is a local maximum in T_c at certain rational values of the magnetic flux per unit cell (including, of course, zero magnetic field), with T_c decreasing linearly in the magnitude of the change of the field away from these special values, as has been observed in experiments on various types of wire grids and Josephson-junction arrays. For the frustrated kagomé grid, on the other hand, there are two bands of lowest-energy states, and the currents in the resulting lowest Landau level of the tight-binding model are instead *paramagnetic* and the state's energy *decreases* linearly in $|B|$. This results in a *minimum* in T_c versus field at the frustrating value of one-half of a flux quantum per triangular plaquette, as is seen experimentally in the kagomé superconducting grids at this frustrating value of the applied field.

Thus from the specific kagomé-lattice tight-binding model, we are led to consider the general case of Landau levels in a small magnetic field with two degenerate bands. In this paper we examine this more general problem first and then show how the kagomé lattice spectrum reduces to a special case, which can be readily solved analytically. We have also obtained extensive numerical results for the kagomé tight-binding spectrum, which agree well with our analytic results. We conclude with a discussion of the kagomé grid superconducting wire networks that motivated this work.

II. TWO-BAND LANDAU LEVELS

Here we will explore a generalization of the usual Landau levels for a charged particle moving in two dimensions in a uniform magnetic field. The new case we consider is where the particle in zero field has two bands that are degenerate at zero momentum. This is the case in the kagomé lattice tight-binding model.

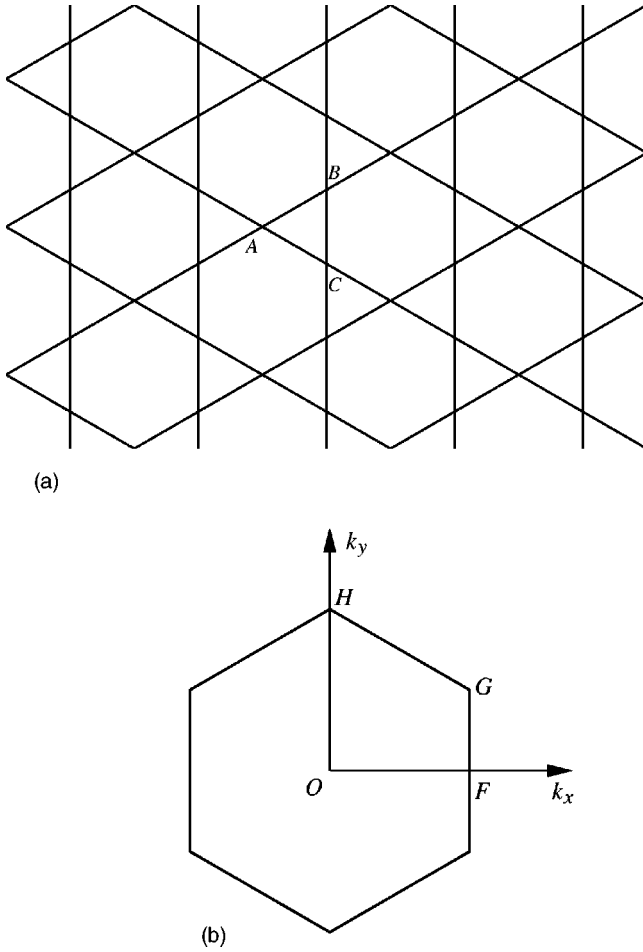


FIG. 1. (a) The kagomé lattice is made up of triangular and hexagonal plaquettes with bond length a . Each unit cell has three sites, denoted here as $A(x, y)$, $B(x + (\sqrt{3}/2)a, y + \frac{1}{2}a)$ and $C(x + (\sqrt{3}/2)a, y - \frac{1}{2}a)$. (b) The first Brillouin zone in reciprocal space. Some points on the edge of the first Brillouin zone: $F(\pi/\sqrt{3}a, 0)$, $G(\pi/\sqrt{3}a, \pi/3a)$, and $H(0, 2\pi/3a)$.

What are the “rules” we will use to generalize the usual one-band case? The particle is moving in two dimensions. We look in the continuum limit of low momentum p , so only look at the energy to order p^2 . At this order in p , the spectrum of the particle’s states in zero magnetic field ($B=0$) is assumed to be isotropic in momentum space, reflecting an underlying system that has at least threefold rotational symmetry. The system is time-reversal invariant for $B=0$ and the spectrum depends only on $|B|$, not on the sign of B . (Because the motion is two dimensional, only the normal component of the magnetic field enters.)

For a single band, the only Hamiltonian that satisfies all these constraints is the usual $H = \Pi^2/(2m^*)$, where

$$\Pi = \mathbf{p} - \frac{q}{c} \mathbf{A} \quad (2.1)$$

is the gauge-invariant momentum. In a small uniform magnetic field, this gives the usual spectrum of equally spaced Landau levels $E_n = \hbar \omega_c (n + \frac{1}{2})$, with $\omega_c = |qB|/(m^*c)$. The currents are diamagnetic for these standard Landau levels.

If instead we have two bands that are degenerate at $\mathbf{p} = 0$ for $B=0$, then in addition to the momentum, the single-particle states are labeled by a band index, which may be treated as a spin 1/2. The general Hamiltonian in this case consists of Hermitian 2×2 (Pauli) matrices operating on the band index and Hermitian quadratic combinations of Π_x and Π_y . In addition to the zero-angular-momentum combination Π^2 that is allowed in the one-band case, there are two Hermitian operators quadratic in Π with angular momentum two: $\Pi_x \Pi_y + \Pi_y \Pi_x$ and $\Pi_x^2 - \Pi_y^2$, as well as the magnetic field itself, which is proportional to the operator combination $i(\Pi_x \Pi_y - \Pi_y \Pi_x)$.

We have a number of constraints that restrict our choice of Hamiltonian; let us first look at the simpler case of $B=0$. The general Hermitian Hamiltonian that is quadratic in \mathbf{p} is

$$H = \sum_{i=0}^3 \sigma_i E_i(\mathbf{p}), \quad (2.2)$$

where the σ_i are the Pauli matrices, with σ_0 the identity matrix, and the E_i are real quadratic functions of \mathbf{p} . This is readily diagonalized, with the resulting eigenenergies

$$E_{\pm}(\mathbf{p}) = E_0 \pm \sqrt{E_1^2 + E_2^2 + E_3^2}. \quad (2.3)$$

Our restriction that the $B=0$ spectrum be rotationally invariant then dictates that $E_0(\mathbf{p}) = d_0 p^2$ and

$$E_1^2 + E_2^2 + E_3^2 = d_2^2 p^4, \quad (2.4)$$

with d_0, d_2 real constants. Another way of writing the Hamiltonian which explicitly breaks it into its parts with orbital angular momentum quantum numbers $m_o = 0, \pm 2$ is

$$H = d_0 \sigma_0 p^2 + \mathbf{z} \cdot \boldsymbol{\sigma} p^2 + (\mathbf{x} - i\mathbf{y}) \cdot \boldsymbol{\sigma} (p_x + ip_y)^2 + (\mathbf{x} + i\mathbf{y}) \cdot \boldsymbol{\sigma} (p_x - ip_y)^2, \quad (2.5)$$

where \mathbf{x}, \mathbf{y} , and \mathbf{z} are real three-vectors in the space spanned by the three Pauli matrices σ_1, σ_2 , and σ_3 . Equation (2.4) requires that these three vectors form a mutually orthogonal triad, with \mathbf{x} and \mathbf{y} being of equal magnitude. Thus we may choose the basis for the band index so that this triad \mathbf{x}, \mathbf{y} , and \mathbf{z} is parallel to the 1, 2, and 3 axes, respectively. This leaves a three-real-parameter family of $B=0$ two-band Hamiltonians

$$H = d_0 \sigma_0 p^2 + d_3 \sigma_3 p^2 + d_1 [\sigma_- (p_x + ip_y)^2 + \sigma_+ (p_x - ip_y)^2], \quad (2.6)$$

where $\sigma_{\pm} = (\sigma_1 \pm i\sigma_2)/2$ are the usual raising and lowering operators. The spectrum is rotationally invariant, as we required:

$$E_{\pm}(\mathbf{p}) = p^2 (d_0 \pm \sqrt{d_1^2 + d_3^2}). \quad (2.7)$$

An important observation about this Hamiltonian, Eq. (2.6), is that it conserves a total angular momentum, provided that we define the particles in the bands to have an “internal” angular momentum whose quantum number $m_i = \pm 1$ is the eigenvalue of σ_3 in this basis. (We will see below that such

an “internal” angular momentum $m_i = \pm 1$ within each unit cell does indeed exist for the low-energy, low-momentum states of the kagomé lattice tight-binding model.) The operators σ_{\pm} then raise and lower the internal angular momentum by two quanta, while $(p_x \pm ip_y)^2$ raise and lower the orbital angular momentum by the same amount. Note that the operators $(p_x \pm ip_y)$ are *not* simply the usual orbital angular momentum raising and lowering operators L_{\pm} ; in addition to changing the orbital angular momentum they also change the radial wave functions. If neither band has negative energy states at $B=0$, so the ground state is at $E=0$, this corresponds to $d_0 \geq \sqrt{d_1^2 + d_3^2} \geq 0$.

Now when we add the uniform magnetic field, the momentum operator \mathbf{p} becomes the gauge-invariant combination $\Pi = \mathbf{p} - (q/c)\mathbf{A}$. For $B \neq 0$ the two components of Π are noncommuting variables with a c -number commutator proportional to the magnetic field:

$$[\Pi_x, \Pi_y] = i \frac{qB\hbar}{c}. \quad (2.8)$$

Thus we can make harmonic-oscillator-type raising and lowering operators a^{\dagger} and a such that

$$\Pi_x = \sqrt{\frac{|qB|\hbar}{2c}}(a^{\dagger} + a) \quad (2.9)$$

and

$$\Pi_y = i \operatorname{sgn}(qB) \sqrt{\frac{|qB|\hbar}{2c}}(a^{\dagger} - a). \quad (2.10)$$

Since the magnetic field itself is quadratic in Π [Eq. (2.8)], a term linear in B may also be added to the Hamiltonian. This term may not contain the identity Pauli matrix, or it will generate a spectrum that is not invariant under inverting B , but it is otherwise unrestricted. Thus we end up with the general two-band Hamiltonian satisfying all our “rules”:

$$H = (d_0\sigma_0 + d_3\sigma_3)\Pi^2 + d_1[\sigma_-(\Pi_x + i\Pi_y)^2 + \sigma_+(\Pi_x - i\Pi_y)^2] + B\mathbf{b} \cdot \boldsymbol{\sigma}, \quad (2.11)$$

where \mathbf{b} is a real three-vector.

At this point let us note that the current density operator for this Hamiltonian,

$$\mathbf{J} = -c \frac{\partial H}{\partial \mathbf{A}}, \quad (2.12)$$

contains, in addition to conventional-looking terms, a term proportional to d_1 that is off diagonal in the band index and linear in the gauge-invariant momentum Π . It is this term that allows Landau levels involving both bands to exhibit paramagnetic currents. These currents arise from an “interference” between the amplitude in one band and the gradient of the amplitude in the other.

The transformation between the Π operators and the raising and lowering operators a and a^{\dagger} is singular at $B=0$, so it is simplest to just consider one sign of qB at a time. In fact it is for $qB < 0$ that the raising and lowering operators a and

a^{\dagger} also raise and lower the orbital angular momentum, so let us do that case. Since we are motivated by superconductors we will take $B > 0$ and $q = -e^* = -2e < 0$. This yields

$$H = B \left[\frac{\hbar e^*}{c} (d_0\sigma_0 + d_3\sigma_3)(2a^{\dagger}a + 1) + \frac{2\hbar e^* d_1}{c} [\sigma_-(a^{\dagger})^2 + \sigma_+ a^2] + \mathbf{b} \cdot \boldsymbol{\sigma} \right]. \quad (2.13)$$

When the one- or two-components of \mathbf{b} are nonzero, this introduces terms that flip the band index without changing the orbital angular momentum and so do not conserve total angular momentum. We have not found a closed-form solution for this general case, but for the kagomé lattice problem we are considering, these terms are not present. In this case, $b_1 = b_2 = 0$, the total angular momentum is conserved. The orbital angular momentum quantum number m_o is also the eigenvalue of the number operator $a^{\dagger}a$ and is restricted to be non-negative for the case $qB < 0$ that we are now considering. Thus for total angular momentum m of 0 or -1 , there is just one state, with internal angular momentum quantum number $m_i = -1$ and $m_o = m + 1$. For $m_i + m_o = m > 0$, on the other hand, there are two states, with $m_i = \pm 1$. If $b_1 = b_2 = 0$ so that m is conserved, the Hamiltonian then reduces to a simple 2×2 matrix. The resulting Landau levels are in general not equally spaced in energy, and even when there are no negative energy states at $B=0$, some of the Landau levels may be at negative energy for $B \neq 0$ and thus paramagnetic. Now will look at the kagomé tight-binding model and show that in the low-momentum limit it realizes this two-band Hamiltonian in the simple case of $d_0 = d_1 > 0$, $d_3 = 0$, and $\mathbf{b} = 0$.

III. KAGOMÉ TIGHT-BINDING SPECTRUM IN ZERO FIELD

The kagomé lattice is a two-dimensional periodic array of corner-sharing triangles with three sites per unit cell. As illustrated in Fig. 1(a), a is the triangle edge length, and A , B , and C denote the three sites in a unit cell. The unit cell can be taken as a rhombus of side $2a$ with angles $2\pi/3$ and $\pi/3$ at its vertices. In reciprocal space $\mathbf{k} = (k_x, k_y)$, the first Brillouin zone is a hexagon with a side length of $2\pi/3a$. Some points on the edge of the first Brillouin zone are shown in Fig. 1(b): $F(\pi/\sqrt{3}a, 0)$ and $G(\pi/\sqrt{3}a, \pi/3a)$, and $H(0, 2\pi/3a)$.

We first consider the tight-binding model for a particle making nearest-neighbor hops on the kagomé lattice in zero magnetic field. The hopping matrix element is $t > 0$. This problem is readily diagonalized. Since there are three sites per unit cell, there are three bands of simultaneous eigenstates of the tight-binding Hamiltonian and the crystal momentum:

$$\begin{aligned} \epsilon_1(\mathbf{k}) &= \epsilon_0 - 2t, \\ \epsilon_{2,3}(\mathbf{k}) &= \epsilon_0 + t \pm t[1 + 4\cos^2(k_y a) \\ &\quad + 4\cos(k_y a)\cos(\sqrt{3}k_x a)]^{1/2}, \end{aligned} \quad (3.1)$$

where ϵ_0 is the on-site energy of the orbitals.

For simplicity, let us set $t=1$ and $\epsilon_0=0$. The spectrum of the second two bands (ϵ_2, ϵ_3) ranges over the interval $[-2, +4]$ and the edges of this interval are reached for $\mathbf{k}=0$. Close to $\mathbf{k}=0$, these two bands are parabolic with an isotropic effective mass. This effective mass is negative $m^* = -\hbar^2/(2ta^2)$ at the top of the upper band at $\epsilon=4$. These two dispersive bands also touch at “Dirac points” at all the corners of the first Brillouin zone [such as G and H in Fig. 1(b)], at energy $\epsilon_2=\epsilon_3=1$.

The first band is completely nondispersive at energy $\epsilon_1 = -2$. Thus the ground state of this particle is highly degenerate. Note also that the bottom of the lower dispersive band is also degenerate with this flat band at $\mathbf{k}=0$. Thus here at $\mathbf{k}=0$ and $\epsilon=-2$ we have two degenerate bands of precisely the type discussed in the previous section of this paper. Since one band is flat, we have $d_0 = \sqrt{d_1^2 + d_3^2}$, in the notation of the previous section. The dispersive band, to quadratic order in the momentum, has energy $\epsilon(\mathbf{k}) - \epsilon(0) = tk^2a^2$, so we have $d_0 = \sqrt{d_1^2 + d_3^2} = ta^2/(2\hbar^2)$.

Some of the degenerate ground states with $\epsilon=-2$ in zero magnetic field are shown in Fig. 2. Figures 2(a) and 2(b) show the states at the Brillouin zone corners, while Figs. 2(c) and 2(d) show the two degenerate states at the zone center with $\mathbf{k}=0$. For small magnetic field, the lowest Landau levels are composed of linear combinations of smooth envelopes times these latter two $\mathbf{k}=0$ states. The two states shown are the eigenstates of the band operator σ_3 . By looking at their wave functions within a unit cell (one triangle) we can see that σ_3 does indeed measure an “internal” angular momentum that has the two possible values $m_i = \pm 1$ in this case, as anticipated above.

We can further anticipate the results of applying a magnetic field by considering just these states. In the absence of coupling between the bands (i.e., for $d_1=0$), the states at the bottom of the bands are Landau quantized in the standard fashion, and their energy thus increases linearly with $|B|$. On the other hand, the degeneracy between the bands is split by the matrix element of the perturbation (d_1) that couples them. In the present case this perturbation is also linearly proportional to $|B|$. Thus whether the lowest-energy states increase or decrease in energy depends on the relative magnitudes of the coupling matrix element and the effective band masses. In terms of currents, a charged particle (here, a Cooper pair) in a given one-band Landau level has a quantized *diamagnetic* dipole moment that is independent of field. Its energy in a field thus increases with $|B|$. For this specific kagomé lattice case, the wave functions *within* one unit cell also have currents and dipole moments as in Figs. 2(c) and 2(d). When these degenerate states are coupled by the perturbation they are admixed and this can produce *paramagnetic* currents. The sum of this and the Landau diamagnetic current can be either diamagnetic or paramagnetic for the lowest-energy state depending on the relative strength of the parameters. In this case we find net paramagnetism in the ground states.

IV. SPECTRUM IN A MAGNETIC FIELD

In the presence of a magnetic field B , the hopping term of the tight-binding Hamiltonian is modified by phase factors

from the vector potential \mathbf{A}^{20} i.e., $t \rightarrow te^{i\gamma_{ij}}$, where γ_{ij} is the phase factor between sites i and j :

$$\gamma_{ij} = \frac{2\pi}{\Phi_0} \int_i^j \mathbf{A} \cdot d\mathbf{l}, \quad (4.1)$$

where $\Phi_0 = hc/e^*$ is the flux quantum.

The (tight-binding) Schrödinger equation in a magnetic field is thus the finite-difference equation

$$\epsilon \phi_i = t \sum_j e^{i\gamma_{ij}} \phi_j, \quad (4.2)$$

where the sum is over all the nearest neighbors of site i . It is convenient to measure the magnetic field in units of the flux quantum per elementary triangular plaquette of the kagomé lattice. The flux through one triangle is $\Phi = (\sqrt{3}/4)Ba^2$. Thus the “filling ratio”—namely, the fraction of a flux quantum through each triangle—is

$$f = \frac{\Phi}{\Phi_0} = \frac{\sqrt{3}}{4} \frac{Be^*a^2}{hc}. \quad (4.3)$$

The flux through an elementary hexagon is 6 times this, $6f\Phi_0$, while the total flux through a unit cell of the kagomé lattice is $8f\Phi_0$.

When f is a rational number that can be written as $8f = k/n$, where k and n are integers with no common factors, the total flux through n unit cells of the kagomé lattice is an integer multiple of Φ_0 . Then with this magnetic field, a gauge can be chosen so that the Hamiltonian has a discrete translational invariance with a unit cell containing n unit cells of the kagomé lattice and thus $3n$ sites. The spectrum of the Hamiltonian then consists of $3n$ bands. These can be obtained numerically for any such rational f (for n not too large); an implementation of this is detailed by Xiao.²¹ The resulting spectrum—namely, the kagomé version of “Hofstadter’s butterfly”—is shown in Fig. 3.

The spectrum has various symmetries: It is only the flux modulo the flux quantum that affects the spectrum, so if f is changed to $f+j$ with j any integer, the spectrum is unchanged. The spectrum is also unchanged on changing f to $-f$, because if ψ is an eigenstate with energy ϵ for field f , then its complex conjugate ψ^* is an eigenstate with the same energy ϵ for field $-f$. These two symmetries are not special to the kagomé lattice. The third symmetry is that if f is changed to $f+\frac{1}{2}$, this is the same as changing t to $-t$, so the spectrum is inverted. Thus the highest-energy states for field near $f=\frac{1}{2}$ are equivalent to the lowest-energy states near zero field. We will look at the behavior near zero field, but because of this last symmetry, what we find also applies near $f=\frac{1}{2}$.

V. LANDAU LEVELS IN THE KAGOMÉ LATTICE NEAR ZERO FIELD

For small magnetic field, the spectrum of the kagomé-lattice tight-binding Hamiltonian shows standard equally spaced Landau levels near the top of the bands, as shown in Fig. 4. Here there is just the one band in zero field, with

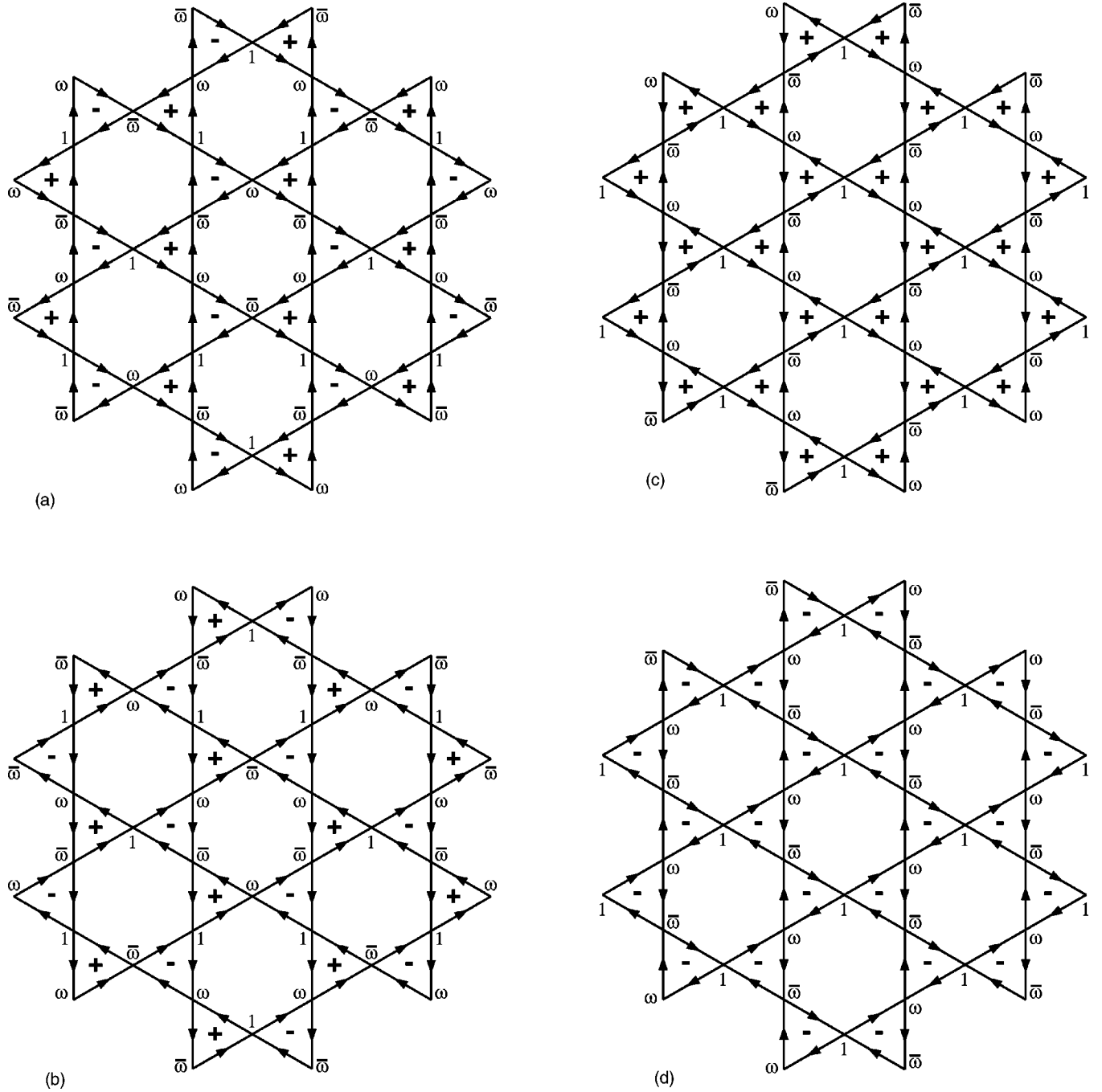


FIG. 2. Some of the degenerate ground states with energy $\epsilon = -2$ in zero magnetic field. $\omega = \exp(i2\pi/3)$ and $\bar{\omega}$ is its complex conjugate. The numbers next to the lattice points indicate the value of the wave function. The arrows along the bonds indicate the currents (supercurrents in the application to superconducting wire networks) and the signs at the centers of the triangles indicate the sign of the circulation of the currents. The $\mathbf{k}=0$ states are (c) and (d).

negative effective mass $m^* = -\hbar^2/(2ta^2)$. The resulting Landau levels, to linear order in the field, should therefore have energy

$$\epsilon = t \left[4 - \frac{16\pi}{\sqrt{3}} |f| \left(n + \frac{1}{2} \right) \right]. \quad (5.1)$$

The numerical results for this portion of the spectrum are shown in Fig. 4 for $f \gtrsim \frac{1}{120}$. The first few Landau levels are

clearly seen, and the asymptotic slopes at small f given by Eq. (5.1) are shown for comparison for the first five Landau levels. At these values of f the fit is not wonderful, but it does seem to be improving with decreasing f , as it should.

More interesting is the bottom of the zero-field spectrum, where there are two degenerate bands. This results in non-standard Landau levels when the field is turned on, as discussed above. An expanded view of this part of the spectrum is shown in Fig. 5. It shows some Landau levels whose en-

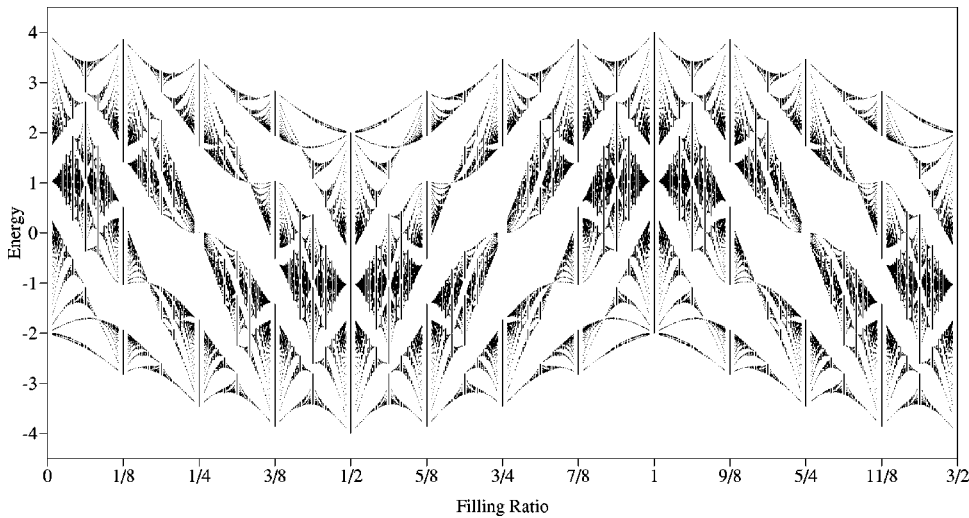


FIG. 3. Spectrum of the kagomé-lattice tight-binding model in a uniform magnetic field. Here and in the following figures the energy is in units of t . The filling ratio f is the fraction of a magnetic flux quantum passing through each elementary triangle of the kagomé lattice.

ergies are increasing linearly with field, as is normal, but these levels are not equally spaced. In addition there are many states whose energies decrease as the field is increased. These latter states are the unusual feature we focus on here. Note that because of the symmetry of the spectrum discussed above, the same features appear at the top of the spectrum near the frustrating value of the magnetic field of $f = 1/2$.

In the one-band case, knowing the effective mass in zero field and the charge is enough to determine the Landau level spectrum to linear order in the magnetic field. For the two-band case, on the other hand [Eq. (2.11)], there is possibly the $B\mathbf{b} \cdot \boldsymbol{\sigma}$ term, which vanishes at zero field, so to determine the values of the three parameters making up \mathbf{b} for the kagomé tight-binding model, we cannot rely only on our knowledge of the zero-field spectrum. So we will now treat the low-momentum behavior to lowest order in the field. What we will find is that $\mathbf{b} = 0$ and $d_3 = 0$.

The unit cell of the kagomé lattice contains three sites around a triangle. We choose a set of three basis states within

this unit cell that respect as much as possible the threefold rotational symmetry of this system about the center of the triangle. The wave function of a state is a complex number defined at each lattice point, but only its gauge-invariant properties are physical. These are the magnitude of the wave function and the *gauge-invariant phase differences* between adjacent lattice points. For any wave function defined at the corners of the triangle in one unit cell, the total gauge-invariant phase difference added up stepping the three steps around the triangle is $2\pi(f + m_i)$, where m_i is an integer. Note m_i measures the state's “internal” angular momentum. The gauge-invariant phase difference between two adjacent lattice points is only well-defined modulo 2π , so let us restrict it to lie in the interval $[-\pi, \pi]$. Thus the three of these phase differences added up must be in the range $[-3\pi, 3\pi]$, and for the small fields f we consider here, this means the total gauge-invariant phase difference around the triangle has to be near one of the three values: -2π , 0 , or

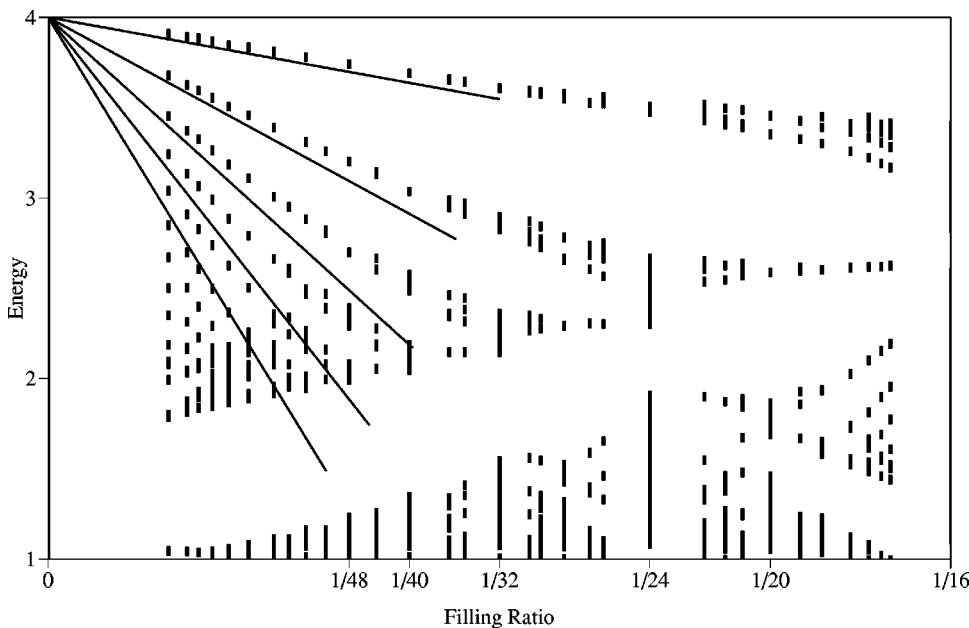


FIG. 4. Energy spectrum for Landau levels near $\epsilon = 4t$. The small- f behavior of the levels corresponding to $n = 0, 1, 2, 3, 4$ is indicated here as solid lines.

2π and m_i is either -1 , 0 or 1 . The basis states we will use are those where the gauge-invariant phase differences are the same along all edges of the triangle, being $2\pi(f+m_i)/3$, while the amplitudes are identical at all three points. In the limit of small momentum and zero field, the upper band near energy $4t$ is made out of the $m_i=0$ states while the lower bands near energy $-2t$ are made out of the two $m_i=\pm 1$ states.

$$H = t \begin{pmatrix} -2 + \Pi^2 + \frac{B}{2} & -i\sqrt{3}(\Pi_x - i\Pi_y) & (\Pi_x - i\Pi_y)^2 \\ i\sqrt{3}(\Pi_x + i\Pi_y) & 4 - 2\Pi^2 & i\sqrt{3}(\Pi_x - i\Pi_y) \\ (\Pi_x + i\Pi_y)^2 & -i\sqrt{3}(\Pi_x + i\Pi_y) & -2 + \Pi^2 - \frac{B}{2} \end{pmatrix}, \quad (5.2)$$

in units where $a=\hbar=1$ and $\Phi_0=2\pi$ and where the rows and columns refer to $m_i = +1, 0, -1$ in that order. Here we have gone to the orders in Π and B that contribute to the spectrum to linear order in $|B|$ and quadratic order in Π . Note that this continuum three-band Hamiltonian conserves total angular momentum. To reduce this to the two-band Hamiltonian for the lowest bands only, we treat the coupling to the upper band in second-order perturbation theory. This eliminates the terms linear in B in the diagonal operators in the above matrix, and the two band Hamiltonian is precisely of the form expected, Eq. (2.11), with $\mathbf{b}=0$, $d_3=0$, and $d_0=d_1=ta^2/(2\hbar^2)$. Finally, the Hamiltonian to this order is simply

$$H = t \left[-2 + \frac{4\pi f}{\sqrt{3}} [\sigma_0(2a^\dagger a + 1) + 2(\sigma_-(a^\dagger)^2 + \sigma_+ a^2)] \right] \quad (5.3)$$

for $f > 0$. This Hamiltonian conserves total angular momentum $m = m_o + m_i$. The resulting Landau level spectrum to linear order in the magnetic field is

$$\epsilon_{\pm} = t \left[-2 + \frac{8\pi}{\sqrt{3}} |f| \left(m + \frac{1}{2} \pm \sqrt{m^2 + m + 1} \right) \right]. \quad (5.4)$$

For $m = -1$ and $m = 0$ there is only the one state with $m_i = -1$, because m_o cannot be negative. (There are no states with $m < -1$.) These states' energies are given by the plus sign in the above equation; they are the two lowest standard one-band Landau levels made out of only the $m_i = -1$ band. Since they are standard one-band Landau levels, they show diamagnetic currents. For $m > 0$, on the other hand, both bands enter and the eigenstates are linear combinations of the $(m+1)$ th Landau level in the $m_i = -1$ band and the $(m-1)$ th Landau level in the $m_i = 1$ band. The interaction between the two bands shifts the energies strongly, with the lower-energy state being pushed to below energy $-2t$. The lowest-energy state of all is the lower-energy (minus sign in the above equation for ϵ_{\pm}) state with $m = 1$, which is at energy

$$\epsilon_{min} = -t \left[2 + 8\pi |f| \left(1 - \frac{\sqrt{3}}{2} \right) \right] \cong -t(2 + 3.37|f|). \quad (5.5)$$

This state is a linear combination of the lowest Landau level ($m_o=0$) in the $m_i=1$ band and the third Landau level ($m_o=2$) in the $m_i=-1$ band. And it is the interference between these two bands that allows this state to be paramagnetic, so its energy decreases with increasing $|B|$.

The straight lines in Fig. 5 correspond to the lowest few of the upper $[+ \text{ in Eq. (5.4)}]$ set of Landau levels. As f is

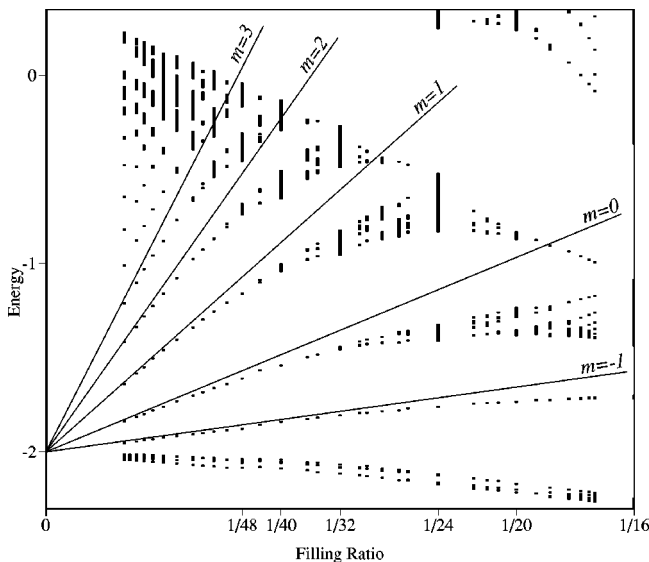


FIG. 5. Lower subband structure close to $\epsilon = -2t$. The calculated small- f behavior of some of the Landau levels is indicated by the straight lines here.

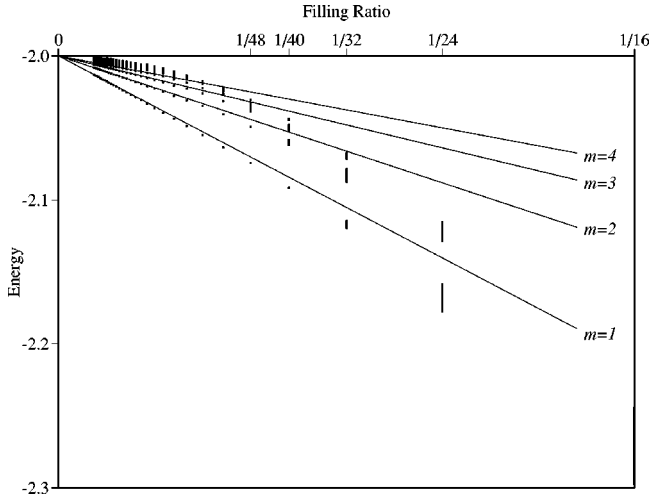


FIG. 6. Subband structure below $\epsilon = -2t$ for filling ratios down to $f = 1/256$. The calculated small- f behavior of the four lowest Landau levels is indicated by the straight lines.

decreased, the numerically obtained bands fit well to these expected Landau levels. A more detailed plot of the lower bands below $\epsilon = -2t$ is shown in Fig. 6, in which this range of the spectrum is calculated for filling ratio from $f = 1/16$ down to $f = 1/256$. For a rational filling ratio $f = 1/8n$, where n is an integer, these lower bands consist of $n - 1$ subbands. Counting the states, we find that in the limit of small magnetic field $1/3$ of all the states are in this set of bands below $\epsilon = -2t$, corresponding to the number of states in the flat $\epsilon = -2t$ band at zero field. The lowest few Landau levels are also indicated by the straight lines in Fig. 6, and again the numerically obtained bands fit well to these as f is reduced.

To examine the very lowest Landau level in more detail, we carried out further numerical calculation of the bottom edge of the spectrum to f as low as $1/840$. These results are shown in Fig. 7 on log-log scales. The straight line corresponds to the small- f behavior, $\Delta\epsilon = 3.37f$, derived above. As can be seen, it gives an excellent fit to the numerical results in this low-field limit.

This behavior in the kagomé lattice is certainly different from the low-field Landau levels of most other periodic

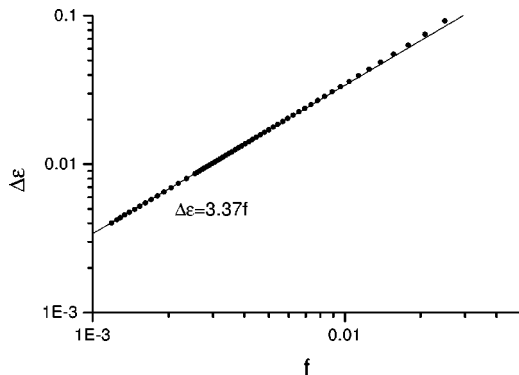


FIG. 7. Log-log plot of the bottom edge of the spectrum close to $\epsilon = -2t$, going down to $f = 1/840$, with $\Delta\epsilon = -2 - (\epsilon_{\min}/t)$. The dots are from the numerics and the straight line indicates the expected small- f behavior.

lattices,^{1,5-7} where the ground-state energy increases as the magnetic field is turned on. In the case of the kagomé lattice, the presence of two degenerate bands in zero field allows these unusual Landau levels to occur.

VI. APPLICATION TO SUPERCONDUCTING WIRE NETWORKS

The network equation for the mean-field phase boundary of a superconducting wire network, derived from linearized Ginzburg-Landau equation, has the same form as that of the tight-binding Schrodinger equation in the same geometry.⁴ For a periodic network with equal bond length a , the superconducting network equation can be expressed as

$$z \cos \frac{a}{\xi} \psi_i = \sum_j \psi_j e^{-i\gamma_{ij}}, \quad (6.1)$$

where ψ_i is the order parameter at site i , ξ is the superconducting coherence length, z is the coordination number of the lattice, and the sum is over all nearest-neighbor sites of i . Compared to the tight binding equation of Eq. (4.2), the correspondence between the two system is given by

$$\frac{\epsilon}{t} \Leftrightarrow z \cos \frac{a}{\xi}. \quad (6.2)$$

The superconducting transition temperature of the network in a magnetic field is given by the upper edge (for $t > 0$) of the tight-binding spectrum. For the kagomé lattice, $z = 4$. The upper edge of the kagomé tight-binding spectrum is plotted in Fig. 8.

For the phase boundary at the lower field limit (small f), our previous discussion of the low-field Landau levels near $\epsilon = 4$ implies a linear relationship between the transition temperature and the magnetic field,

$$\Delta T_c(f) \sim \left(\frac{a}{\xi} \right)^2 \sim |f|, \quad (6.3)$$

where $\Delta T_c(f) = T_c(0) - T_c(f)$ is the suppression of the critical temperature from its zero-field value.

As shown in Fig. 8, strong maxima or minima in the superconducting phase boundary appear at magnetic fields $f = p/8$ for each integer p , which correspond to p magnetic flux quanta through each unit cell. At each of these fields, the tight-binding model is equivalent to a model in zero magnetic field with the hopping matrix elements within each unit cell being complex. Since there are three sites per unit cell, in each case there are three bands in the spectrum. When the magnetic field is changed slightly to $f = p/8 + \Delta f$, the small added magnetic field (of either sign) splits these bands into Landau levels, just like near $f = 0$. For all of these fields, except the special case $f = 1/2$, the upper edge of the spectrum is a state at crystal momentum zero in a nondegenerate band. Thus changes in the magnetic field produce conventional Landau levels like near $f = 0$. This causes the upper edge of the spectrum to decrease linearly in $|\Delta f|$, resulting in a local *maximum* in the superconductor's transition temperature versus field at those fields. The appearance of a local

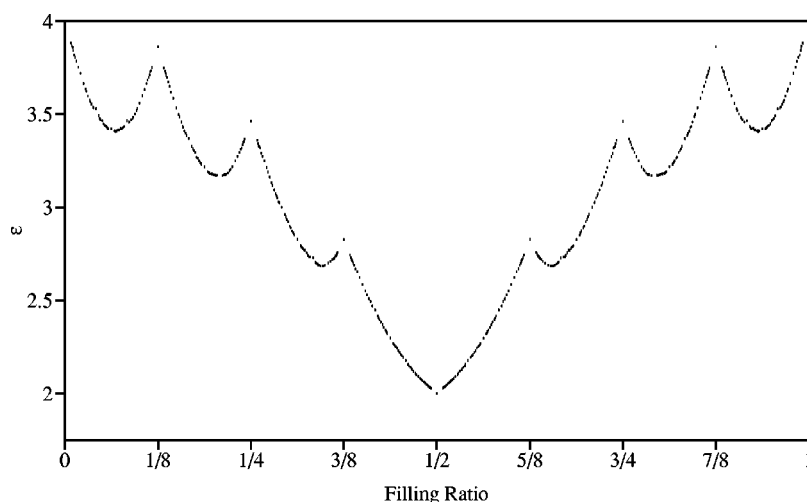


FIG. 8. Upper edge of the kagomé-lattice tight-binding spectrum for $t > 0$. The mean-field transition temperature T_c of a kagomé wire-grid superconductor is linearly related to ϵ , so T_c has a minimum at filling ratio $f = 1/2$.

minimum in T_c at $f = 1/2$ is due to the special degeneracy in the highest band that occurs due to the magnetic frustration at that field, resulting in Landau levels whose energy moves linearly away from the band center as the field is changed from this special value, as discussed above.

A local minimum in T_c versus field also occurs at $f = 1/2$ in the so-called T_3 or dice lattice,^{7,8} but for quite different reasons from the kagomé lattice case. The dice lattice is the dual to the kagomé lattice. Its elementary plaquettes are all rhombuses, and f is the number of flux quanta passing through each such rhombic plaquette. Like the kagomé lattice, the dice lattice has three sites per unit cell. At $f = 1/2$ in this dice lattice, the spectrum consists of three dispersionless (infinite mass) bands,⁷ with no degeneracy between the bands. For the dice lattice, the linear dependence of the upper edge of the spectrum on field near $f = 1/2$ arises not from the formation of Landau levels, but from an “orbital Zeeman effect.” States with nonzero net magnetic moments of either

sign and localized to just a few lattice sites can be formed out of the highest-energy states at $f = 1/2$. The magnetic moments are due to currents circulating around the plaquettes and cause these states to have energies that depend linearly on the magnetic field. Although the kagomé lattice spectrum also has such a dispersionless band at $f = 1/2$, the localized states that can be made from this band in the kagomé case have no net magnetic moment and thus no such orbital Zeeman effect.

ACKNOWLEDGMENTS

We thank Duncan Haldane, Mark J. Higgins, Shobo Bhattacharya, Kyungwha Park, Marc Schreiber, Yeong-Lieh Lin, and Franco Nori for helpful discussions. This work was supported by NSF Grant Nos. DMR 98-09483, 98-02468, 99-76576, and 02-13706.

¹D. R. Hofstadter, Phys. Rev. B **14**, 2239 (1976).

²B. Pannetier, J. Chaussy, and R. Rammal, J. Phys. (Paris) **44**, L853 (1983).

³See, for instance, *Coherence in Superconducting Networks*, edited by J. E. Mooij and G. B. J. Schöen, Physica B **152**, 1 (1988).

⁴S. Alexander, Phys. Rev. B **27**, 1541 (1983).

⁵F. H. Claro and G. H. Wannier, Phys. Rev. B **19**, 6068 (1979).

⁶R. Rammal, J. Phys. (Paris) **46**, 1345 (1985).

⁷J. Vidal, R. Mosseri, and B. Douçot, Phys. Rev. Lett. **81**, 5888 (1998).

⁸B. Pannetier, C. C. Abilio, E. Serret, Th. Fournier, P. Butaud, and J. Vidal, Physica C **352**, 411 (2001).

⁹V. Elser, Phys. Rev. Lett. **62**, 2405 (1989).

¹⁰I. Ritchey, P. Chandra, and P. Coleman, Phys. Rev. B **47**, 15 342 (1993).

¹¹J. T. Chalker, P. C. W. Holdsworth, and E. F. Shender, Phys. Rev. Lett. **68**, 855 (1992).

¹²D. A. Huse and A. D. Rutenberg, Phys. Rev. B **45**, 7536 (1992).

¹³J. N. Reimers and A. J. Berlinsky, Phys. Rev. B **48**, 9539 (1993).

¹⁴J. Villain, R. Bidaux, J. P. Carton, and R. Conte, J. Phys. (Paris) **41**, 1263 (1980).

¹⁵D. S. Greywall and P. A. Busch, Phys. Rev. Lett. **62**, 1868 (1989).

¹⁶D. S. Greywall and P. A. Busch, Phys. Rev. Lett. **65**, 2788 (1990).

¹⁷For a brief review of this work, see A. P. Ramirez, J. Appl. Phys. **70**, 5952 (1991).

¹⁸M. J. Higgins, Y. Xiao, S. Bhattacharya, P. M. Chaikin, S. Sethuraman, R. Bojko, and D. Spencer, Phys. Rev. B **61**, R894 (2000); Y. Xiao, D. A. Huse, P. M. Chaikin, M. J. Higgins, S. Bhattacharya, and D. Spencer, *ibid.* **65**, 214503 (2002).

¹⁹Y.-L. Lin and F. Nori, Phys. Rev. B **50**, 15 953 (1994); **65**, 214504 (2002).

²⁰R. E. Peierls, Z. Phys. **80**, 763 (1933).

²¹Yi Xiao, Ph.D. thesis, Princeton University, 2000.